

## EFFECT OF THE DRAG FORCE ON THE ORBITAL MOTION OF THE BROAD-LINE REGION CLOUDS

FAZELEH KHAJENABI

Department of Physics, Faculty of Sciences, Golestan University, Gorgan 49138-15739, Iran  
f.khajenabi@gu.ac.ir*Draft version May 31, 2016*

## ABSTRACT

We investigate orbital motion of cold clouds in the broad line region of active galactic nuclei subject to the gravity of a black hole and a force due to a nonisotropic central source and a drag force proportional to the velocity square. The intercloud is described using the standard solutions for the advection-dominated accretion flows. Orbit of a cloud decays because of the drag force, but the typical time scale of falling of clouds onto the central black hole is shorter comparing to the linear drag case. This time scale is calculated when a cloud is moving through a static or rotating intercloud. We show that when the drag force is a quadratic function of the velocity, irrespective of the initial conditions and other input parameters, clouds will generally fall onto the central region much faster than the age of whole system and since cold clouds present in most of the broad line regions, we suggest that mechanisms for continuous creation of the clouds must operate in these systems.

*Subject headings:* galaxies: active - galaxies: nuclei

## 1. INTRODUCTION

Emission of broad-line region (BLR) of active galactic nuclei (AGNs) is explained by models which propose continuous steady flows or presence a very large number of clouds which exhibit some bulk motion (e.g., Osterbrock & Mathews 1986; Netzer 2013; Rees 1987; Rees et al. 1989). In the early models for the BLRs, the clouds are moving inward or outward through a static or slowly moving background gas (e.g., Mathews 1974; Blumenthal & Mathews 1975, 1979). Subsequent studies showed that the clouds may exhibit orbital motion under the strong gravitational potential of a central object. Kwan & Carroll (1982) constructed a kinematic model in which the BLR clouds orbit the central object in nearly parabolic orbits and this model has been extended by Carroll & Kwan (1985) to include the effects of a finite infalling cloud number and size. There are considerable uncertainties about formation of the BLR clouds and their dynamical stability (e.g., Mathews 1986; Mathews & Veilleux 1989), however, many authors have successfully produced emission of BLR systems based on the discrete cloud concept (e.g., Capriotti et al. 1979, 1980, 1981; Fromerth & Melia 2001; Netzer & Marziani 2010).

Most of these models assume that the BLR clouds are pressure-confined, though a few authors argue that the clouds are transient rather than stable long-lived objects. Orbital motion of the BLR clouds is a rich source of information to estimate the mass of the central black hole. While early models are considering gravitational force of the central black hole as a dominant force, it has been argued that BLR clouds are also subject to a force due to the intense radiation of a central source (e.g., an accretion disc) and the mass of the central black hole is underestimated if radiation pressure is neglected (e.g., Marconi et al. 2008; Namekata et al. 2014). Moreover, it has been suggested that the central radiation is nonisotropic (Liu & Zhang 2011) and the orbits of BLR clouds are significantly modified when this feature of radiation is considered (Plewa et al. 2013; Khajenabi

2015).

Clouds embedded in a hot gaseous medium have also been discovered near to the Galactic center (Gillesen et al. 2012). These low-mass gas clouds, known as G1 and G2, are moving on highly eccentric orbits through gaseous medium around a central black hole. Using orbital motions of these clouds, one can probe the accretion flow feeding Sgr A\* (McCourt & Madigan 2015; Pfuhl et al. 2015). There are considerable uncertainties about the true nature of intercloud medium and physical mechanisms that may lead to the formation of these clouds. Although various processes have been proposed for the formation of G1 and G2 or BLR clouds, we don't yet know for sure if these clouds are formed as a result of such mechanisms. The intercloud medium of G1 and G2 is described, however, successfully using a kind of accretion flow which is known as Advection-Dominated Accretion Flow (ADAF; Narayan & Yi 1994). It is a good motivation to assume that BLR clouds are also moving through this type of accretion flows (Krause et al. 2011). Nevertheless, most of the previous semi-analytical studies of BLR clouds' dynamics prescribe pressure profile of the intercloud medium as a simple power-law function of the radial distance (e.g., Netzer & Marziani 2010; Krause et al. 2011, 2012; Plewa et al. 2013; Khajenabi 2015).

Since each BLR cloud is assumed to be in a pressure-confined state, its radius is determined by a balance between the interior pressure of a cloud and its ambient pressure. Then, orbital motion of a BLR cloud is treated like a classical two-body problem where a cloud with a fixed mass is subject to the central gravity and a force due to the radiation. Most of the previous analytical studies of BLR cloud's dynamics actually follow this approach.

Netzer & Marziani (2010) studied orbital motion of pressure-confined BLR clouds in AGNs considering the combined influence of the central gravity and the radiation pressure. A modified estimate for the mass of the central black hole is presented according to their orbital

analysis. Krause et al. (2011) addressed stability of the orbits using analytical calculations for both isotropic and anisotropic light sources and found that stable orbits may exist under certain circumstances. Although it is unlikely to obtain analytical solutions for the orbital motion of BLR clouds under general conditions, an interesting analytical solution for the orbit of BLR clouds with a fixed column density has been obtained by Plewa et al. (2013). In all these works, the intercloud is a simple power-law prescription not based on a physically supported model. Moreover, variations of the intercloud's pressure profile with the polar angle has been neglected. These issues motivated Khajenabi (2015) to study orbital motion of BLR clouds through an ADAF atmosphere where its pressure profile is based on a two-dimensional self-similar analytical solution for ADAFs (Shadmehri 2014). Under these conditions it was shown that stability of the orbits implies that the ensemble of clouds tends to have a disc like configuration.

None of the above studies about orbital motion of BLR clouds considered interaction of the clouds with the surrounding gas via a drag force. As for the G1 and G2 clouds, recent studies show that the drag force has a vital role in the orbits of these clouds (e.g., McCourt & Madigan 2015; Pfuhl et al. 2015). Just recently, Shadmehri (2015) studied orbits of BLR clouds subject to a drag force proportional to the velocity. For a particular set of the input parameters, Shadmehri (2015) presented an analytical solution for the orbits of the clouds which reduces to the analytical solution of Plewa et al. (2013) in the absence of the drag force. In the presence of the drag force, irrespective of the input parameters, orbit of a BLR cloud would decay in a way that it will eventually fall onto the central region. According to the arguments of Shadmehri (2015) if the time that takes a cloud to reach from its initial position to the central part, or time-of-flight, becomes less than the lifetime of the whole system, then BLR clouds are transient structures rather than long-lived objects so that mechanisms for continually forming BLR clouds are needed. In other words, drag force implies a physical constraint for analyzing orbits of the clouds. Shadmehri (2015) found that time-of-flight of a BLR cloud is proportional to the inverse of the dimensionless drag coefficient and using this relation he showed that time-of-flight is indeed shorter than the lifetime of the whole system for a wide range of the input parameters. This interesting finding implies existence of mechanisms for continuously forming these clouds.

However, there are caveats regarding to the analysis of Shadmehri (2015). First of all, in his study the drag force is proportional to the velocity which is valid as long as the intercloud is laminar. Although he argues that Reynolds number is less than one which confirms the adopted drag force, for some other input parameters one can easily show that Reynolds number could be much larger than one. Introducing Reynolds number as  $Re = \rho v L / \mu$ , it can be rewritten as  $Re = 2(v/\bar{u})(L/\lambda)$ , where  $\rho$ ,  $v$ ,  $L$ ,  $\mu$ ,  $\bar{u}$  and  $\lambda$  are the density of gas, the mean velocity of the cloud relative to the gas, characteristic length, dynamic viscosity, the average molecular speed and the mean free path, respectively. If the number density of the intercloud gas is  $10^4 \text{ cm}^{-3}$  and its average temperature is  $10^8 \text{ K}$ , then we have  $\bar{u} \approx 2 \times 10^6 \text{ m s}^{-1}$  and  $\lambda \approx 10^{10} \text{ m}$ . The

Keplerian velocity at the radial distance 1 pc from the central mass  $10^6$  solar mass is around  $6.5 \times 10^4 \text{ m s}^{-1}$ . If we adopt velocity of a cloud approximately equal to this Keplerian velocity and for a typical length  $10^{13} \text{ cm}$ , the Reynolds number becomes around 0.65. Obviously, if the typical length is taken larger, say  $10^{15} \text{ cm}$ , then we have  $Re = 65$ . Also, for a more massive central mass, the Reynolds number is larger than unity. It means that the intercloud medium is turbulent and the drag force should be taken in proportion to the velocity square. In the present work, we plan to study orbits of BLR clouds with a quadratic drag force. At variance with previous work, nevertheless, the intercloud is prescribed using the standard ADAF solutions. Under these circumstances, we calculate time-of-flight of the clouds to see if the main finding of Shadmehri (2015) is still valid when the drag force is a quadratic function of the velocity. Moreover, in most previous studies, the background gas is assumed to be in a static configuration. We also consider rotation of the medium which a cloud moves through it. In next section, we present basic assumptions and the orbital equations. In section 3, time-of-flight is calculated numerically. We then conclude with our main findings in section 4.

## 2. GENERAL FORMULATION

### 2.1. Basic Assumptions

We study orbital motion of a BLR cloud with mass  $m$  subject to three main forces, i.e. gravitational force of a central black hole with mass  $M$ , a non-isotropic force due to the radiation of a central accretion disc (Liu & Zhang 2011), and a drag force in the opposite direction of the BLR orbital motion. Under these circumstances, direction of cloud's angular momentum is conserved, though its magnitude gradually decreases because of the resistive force. Therefore, motion of a BLR cloud will be in a plane where its inclination  $i$  is fixed by the initial angular momentum and it is an input parameter in our model. A system of coordinates  $(x, y, z)$  is constructed so that the central black hole locates at its origin and the central radiating thin accretion is at  $z = 0$  plane (Figure 1). Thus, location of a cloud in its orbit with inclination angle  $i$  with respect to the  $x - y$  plane is uniquely determined by its distance  $r$  from the origin and the polar angle  $\theta$ . The cloud orbit intersects the  $x - y$  (disk) plane at the ascending node  $A$  so that we define the angle  $\angle AOC = \psi$ . Having the inclination angle  $i$ , position of a cloud is determined by  $r$  and  $\psi$ .

Geometrical shape of a BLR cloud is assumed to be spherical, for simplicity. Moreover, the clouds are considered to be optically thick. But since the clouds are pressure-confined by definition, physical properties of the ambient gaseous medium like its pressure profile determines how the radius of a cloud varies depending on its position in orbital motion. There are considerable uncertainties about the true nature of intercloud medium. In other words, irrespective of the confinement mechanisms, internal pressure of a cloud is in balance with the ambient pressure.

Since each cloud is in pressure equilibrium with the hot background gas, its radius becomes  $R_{cl} \propto P_{gas}^{-1/3}$  where  $P_{gas}$  is the intercloud gas pressure. On the other hand, according to the standard similarity solutions for

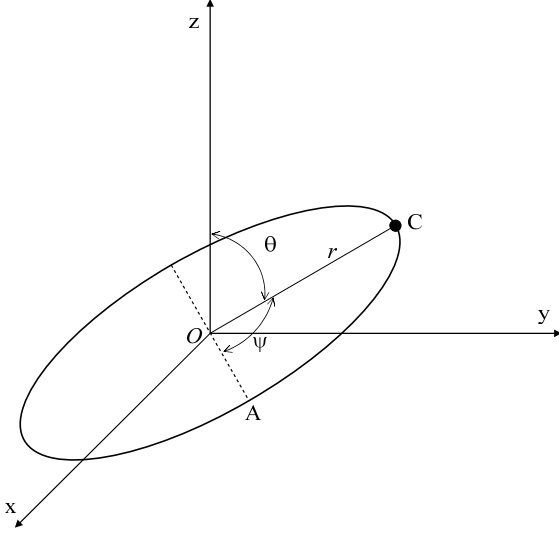


FIG. 1.— The central black hole locates at origin  $O$  and position of the cloud  $C$  is determined by the radial distance  $r$  and the polar angle  $\theta$  and the inclination angle of the orbital plane. Since direction of the angular momentum is conserved, the orientation of the orbital plane is fixed and its intersection with the  $x-y$  plane is denoted by  $OA$ . Thus, position of the cloud  $C$  is equivalently determined by the radial distance  $r$  and the angle  $\angle AOC = \psi$ .

ADAFs (Narayan & Yi 1994), the pressure distribution is proportional to a power-law function of the radial distance as  $P_{\text{gas}} \propto r^{-s}$  where  $s$  is  $5/2$ . Therefore, we can rewrite radius of a single cloud as a function of its location, i.e.

$$R_{\text{cl}} = R_{\text{cl}0} \left( \frac{r}{r_0} \right)^{5/6}, \quad (1)$$

where  $r_0$  is the initial radial distance of the cloud, and  $R_{\text{cl}0}$  is the radius of the cloud at  $r_0$ . We can calculate the column density  $N_{\text{cl}} = 3m/2\mu_m m_p A$ , where  $\mu_m$  is the mean molecular weight and  $A$  is cross section of a cloud. Having the above relations for  $R_{\text{cl}}$  and  $P_{\text{gas}}$ , the column density of a pressure-confined cloud becomes  $N_{\text{cl}} \propto P_{\text{gas}}^{2/3}$  or  $N_{\text{cl}} = N_0 (r/r_0)^{-5/3}$  where  $N_0 = 3m/(2\mu_m m_p \pi R_{\text{cl}0}^2)$  is a constant column density. Also, the density of gas in the standard ADAF similarity solution is written as a power-law function of the radial distance, i.e.

$$\rho = \rho_0 \left( \frac{r}{r_0} \right)^{-3/2}, \quad (2)$$

where  $\rho_0$  is the mass density of the intercloud gas at radius  $r_0$ . We adopt the outer radius of the system as  $r_0$  with a value between 0.01 pc to 1 pc and the number density is  $n_0 \sim 10^4 \text{ cm}^{-3}$  according to the observations (e.g., Rees et al. 1989; Netzer 2013; Marconi et al. 2008; Plewa et al. 2013).

The radial velocity  $v_r$  and the rotational velocity  $v_\varphi$

of an ADAF are also power-law function of the radial distance. Similarity solutions of Narayan & Yi (1994) are written  $v_r = -v_{0r} v_K$  and  $v_\varphi = v_{0\varphi} v_K$ , where  $v_K = \sqrt{GM/r}$  is Keplerian velocity and the coefficients  $v_{0r}$  and  $v_{0\varphi}$  are obtained as,

$$v_{0r} = (5 + 2\varepsilon') \frac{g(\alpha, \varepsilon')}{3\alpha}, \quad (3)$$

and

$$v_{0\varphi} = \sqrt{\frac{2\varepsilon'(5 + 2\varepsilon')}{9\alpha^2}} g(\alpha, \varepsilon'). \quad (4)$$

Here, we have

$$g(\alpha, \varepsilon') = \sqrt{1 + \frac{18\alpha^2}{(5 + 2\varepsilon')^2}} - 1, \quad (5)$$

where  $\alpha$  is the standard Shakura-Sunyaev viscosity parameter for modeling ADAF's turbulence. Moreover, the parameter  $\varepsilon'$  is written as  $\varepsilon' = \varepsilon/f$  where  $\varepsilon = (5/3 - \gamma)/(\gamma - 1)$ , and  $\gamma$  is the ratio of specific heats and the parameter  $f$  measures the amount of the advected energy. For example, in a fully advective flow with  $\alpha = 0.1$  and  $\varepsilon' = 1$ , we obtain  $v_{0r} \simeq 0.04$  and  $v_{0\varphi} \simeq 0.53$ .

## 2.2. Equations of Motion in a Static Atmosphere

We can now write equations of motion of a cloud which is under the influence of the three main forces: the gravitational force of the central mass,  $\mathbf{F}_{\text{grav}}$ , a force due to non-isotropic radiation of the central accretion disc (Liu & Zhang 2011),  $\mathbf{F}_{\text{rad}}$ , and a drag force proportional to the velocity square in the opposite direction of the cloud's motion,  $\mathbf{F}_{\text{drag}}$ . These forces can be written as

$$\mathbf{F}_{\text{grav}} = -\frac{GMm}{r^2} \mathbf{e}_r, \quad (6)$$

$$\mathbf{F}_{\text{rad}} = \frac{A}{c} \frac{L_a}{2\pi r^2} |\cos \theta| \mathbf{e}_r, \quad (7)$$

$$\mathbf{F}_{\text{drag}} = -\frac{1}{2} \rho C_D A |\mathbf{v}| \mathbf{v}, \quad (8)$$

where  $A$  is the cross sectional area of a cloud and  $L_a$  is the luminosity of the central source. In the above equation for the drag force,  $C_D$  is the drag coefficient which depends on the shape of the cloud and even Reynolds number (e.g., McCormick 1979). For a sphere, value of  $C_D$  may vary from large values for laminar flow to 0.47 for turbulent flow (McCormick 1979).

It is more convenient to re-write the force due to the radiation in terms of the column density  $N_{\text{cl}}$  and the Eddington ratio  $l = L_a/L_{\text{edd}}$ , where  $L_{\text{edd}} = 4\pi GM m_p c / \sigma_T$  is the Eddington luminosity. Here,  $\sigma_T$  is the Thompson cross-section. Thus, the force due to the radiation becomes

$$\mathbf{F}_{\text{rad}} = \frac{GMm}{r^2} \frac{3l}{\mu_m N_{\text{cl}} \sigma_T} |\cos \theta| \mathbf{e}_r, \quad (9)$$

or

$$\mathbf{F}_{\text{rad}} = \frac{GMm}{r^2} k |\sin \psi| \mathbf{e}_r, \quad (10)$$

where the dimensionless parameter  $k$  is defined as

$$k = \frac{3l}{\mu_m N_{\text{cl}} \sigma_T} \sin(i). \quad (11)$$

Substituting radial dependence of the column density, the parameter  $k$  becomes  $k = k_0(r/r_0)^{5/3}$  where  $k_0 = 3l \sin(i)/\mu_m N_0 \sigma_T$ .

Most of previous authors assume that the intercloud is static which means the background gas does not move. Thus, the relative velocity of a cloud with respect to its ambient medium is cloud's velocity itself. We first consider this simplified situation. Thus, equations of the orbital motion are written as

$$\ddot{r} - r\dot{\psi}^2 = \frac{GM}{r^2} (k|\sin \psi| - 1) - \frac{\rho C_D A}{2} \dot{r} \sqrt{\dot{r}^2 + r^2 \dot{\psi}^2}, \quad (12)$$

$$r\ddot{\psi} + 2\dot{r}\dot{\psi} = -\frac{\rho C_D A}{2} r\dot{\psi} \sqrt{\dot{r}^2 + r^2 \dot{\psi}^2}, \quad (13)$$

where  $\dot{r} = dr/dt$ ,  $\ddot{r} = d^2r/dt^2$  and  $\dot{\psi} = d\psi/dt$ . Note that the temperature of a cloud during its orbital motion is almost constant.

The above orbital equations (12) and (13) are now written in the non-dimensional forms which are more convenient for the numerical integration. Thus, we use the initial radial distance  $r_0$  as a reference length scale. Then, Keplerian velocity at this radial distance is written as  $v_K(r_0) = \sqrt{GM/r_0}$  and our unit time becomes  $t_0 = r_0/v_K(r_0)$ . We now change the variables as  $r = r_0 \tilde{r}$  and  $t = t_0 \tau$ . Thus, equations (12) and (13) become

$$\ddot{\tilde{r}} - \tilde{r}\dot{\psi}^2 = \frac{1}{\tilde{r}^2} \left( k_0 \tilde{r}^{5/3} |\sin \psi| - 1 \right) - \beta \dot{\tilde{r}} \tilde{r}^{1/6} \sqrt{\dot{\tilde{r}}^2 + \tilde{r}^2 \dot{\psi}^2}, \quad (14)$$

and

$$\tilde{r}\ddot{\psi} + 2\dot{\tilde{r}}\dot{\psi} = -\beta \dot{\psi} \tilde{r}^{7/6} \sqrt{\dot{\tilde{r}}^2 + \tilde{r}^2 \dot{\psi}^2}, \quad (15)$$

where  $\dot{\tilde{r}} = d\tilde{r}/d\tau$ ,  $\ddot{\tilde{r}} = d^2\tilde{r}/d\tau^2$  and  $\dot{\psi} = d\psi/d\tau$ . The dimensionless drag coefficient is denoted by  $\beta$ , i.e.

$$\beta = \frac{3}{8} C_D \left( \frac{r_0}{R_{cl0}} \right) \left( \frac{\rho_0}{\rho_{cl0}} \right). \quad (16)$$

In writing the above equations, we assume that the mass of cloud is conserved during its orbital motion. We note that radius of a cloud and its density at the distance  $r_0$  are denoted by  $R_{cl0}$  and  $\rho_{cl0}$ , respectively. Equations (14) and (15) are our main equations for determining orbit of a cloud in a static atmosphere when the drag force is proportional to the velocity square. In section 3, we solve these equations to analyze orbits of a cloud.

### 2.3. Equations of Motion in a Rotating Atmosphere

We now consider a more realistic situation where the ambient gas is rotating and has radial velocity according to equations (3) and (4). In writing the drag force, then, the relative velocity is considered. Thus, orbital equations become

$$\ddot{r} - r\dot{\psi}^2 = \frac{GM}{r^2} (k|\sin \psi| - 1) - \frac{\rho C_D A}{2} \times \sqrt{(\dot{r} + v_{0r} v_K)^2 + (r\dot{\psi} - v_{0\phi} v_K)^2}, \quad (17)$$

$$r\ddot{\psi} + 2\dot{r}\dot{\psi} = -\frac{\rho C_D A}{2} \times (r\dot{\psi} - v_{0\phi} v_K) \sqrt{(\dot{r} + v_{0r} v_K)^2 + (r\dot{\psi} - v_{0\phi} v_K)^2}. \quad (18)$$

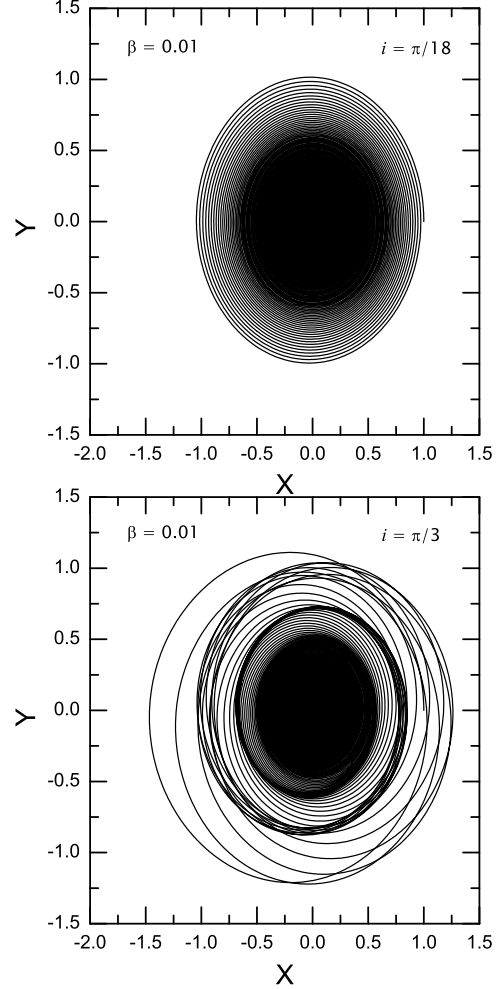


FIG. 2.— Orbit of a BLR cloud in the plane of motion with inclination angles  $i = \pi/18$  (top) and  $i = \pi/3$  (bottom) for  $\beta = 0.01$ . The other input parameters are  $\alpha = 0.1$ ,  $\epsilon' = 1$ ,  $\mu_m N_0 \sigma_T = 3/2$  and  $l = 0.1$ . Initial conditions are  $\tilde{r}(\tau = 0) = 1$ ,  $\dot{\tilde{r}}(\tau = 0) = 0$ ,  $\psi(\tau = 0) = 0$  and  $\dot{\psi}(\tau = 0) = 1$ .

Again, it is more convenient to use non-dimensional equations instead of the above orbital equations. So, we transform equations (17) and (18) to the following non-dimensional forms:

$$\begin{aligned} \ddot{\tilde{r}} - \tilde{r}\dot{\psi}^2 &= \frac{1}{\tilde{r}^2} \left( k_0 \tilde{r}^{5/3} |\sin \psi| - 1 \right) - \beta \times \\ &(\dot{\tilde{r}} + v_{0r} \tilde{r}^{-1/2}) \tilde{r}^{1/6} \sqrt{(\dot{\tilde{r}} + v_{0r} \tilde{r}^{-1/2})^2 + (\tilde{r}\dot{\psi} - v_{0\phi} \tilde{r}^{-1/2})^2}, \\ \tilde{r}\ddot{\psi} + 2\dot{\tilde{r}}\dot{\psi} &= -\beta \times \\ &(\dot{\psi} - v_{0\phi} \tilde{r}^{-3/2}) \tilde{r}^{7/6} \sqrt{(\dot{\tilde{r}} + v_{0r} \tilde{r}^{-1/2})^2 + (\tilde{r}\dot{\psi} - v_{0\phi} \tilde{r}^{-1/2})^2}, \end{aligned} \quad (19)$$

where dimensionless parameter  $\beta$  is defined in equation (16). The above equations are solved subject to the appropriate initial conditions in the next section.

## 3. ANALYSIS

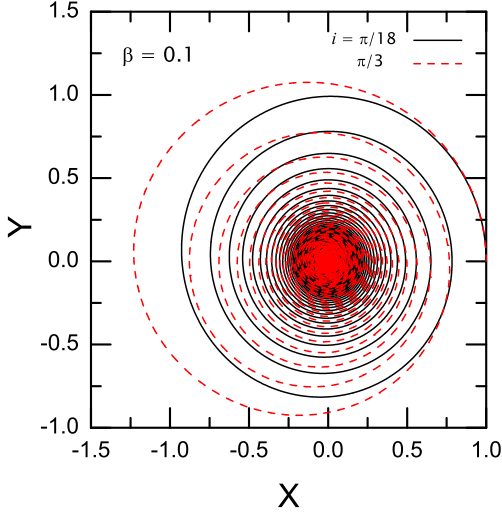


FIG. 3.— Same as Figure 2, but with inclination angles  $i = \pi/18$  (solid) and  $i = \pi/3$  (dashed) and a larger dimensionless drag coefficient, i.e.  $\beta = 0.1$ .

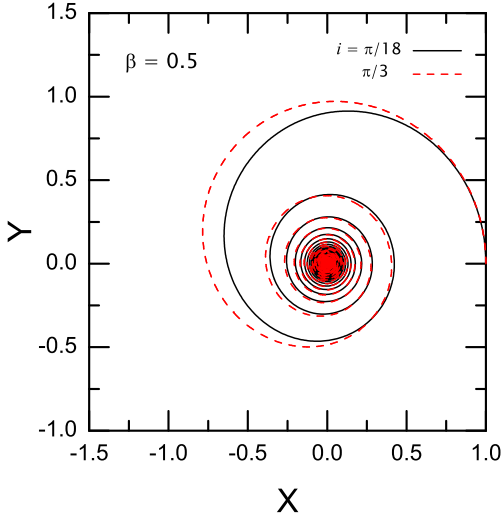


FIG. 4.— Same as Figure 2, but with inclination angles  $i = \pi/18$  (solid) and  $i = \pi/3$  (dashed) and a larger dimensionless drag coefficient, i.e.  $\beta = 0.5$ .

TABLE 1

OUR INPUT PARAMETER FOR DESCRIBING A BLR CLOUD AND ITS AMBIENT GAS AND THE RESULTING DIMENSIONLESS DRAG COEFFICIENT. NOTE THAT EACH ROW CORRESPONDS TO A CLOUD WITH A CERTAIN MASS.

$r_0$	$n_0$	$R_{cl0}$	$n_{cl0}$	$\beta/C_D$
1 pc	$10^4 \text{ cm}^{-3}$	$10^{14} \text{ cm}$	$10^{10} \text{ cm}$	$1.15 \times 10^{-2}$
1 pc	$10^4 \text{ cm}^{-3}$	$10^{12} \text{ cm}$	$10^{10} \text{ cm}$	1.15
0.01 pc	$10^4 \text{ cm}^{-3}$	$10^{14} \text{ cm}$	$10^{10} \text{ cm}$	$1.15 \times 10^{-4}$
0.01 pc	$10^4 \text{ cm}^{-3}$	$10^{12} \text{ cm}$	$10^{10} \text{ cm}$	$1.15 \times 10^{-2}$

TABLE 2

SAME AS TABLE 1, BUT EACH ROW CORRESPONDS TO A BLR CLOUD WITH A MASS EQUAL TO  $10^{-8}$  SOLAR MASS.

$r_0$	$n_0$	$R_{cl0}$	$n_{cl0}$	$\beta/C_D$
1 pc	$10^4 \text{ cm}^{-3}$	$10^{14} \text{ cm}$	$4.6 \times 10^6 \text{ cm}$	25
1 pc	$10^4 \text{ cm}^{-3}$	$10^{12} \text{ cm}$	$4.6 \times 10^{12} \text{ cm}$	$2.5 \times 10^{-3}$
0.01 pc	$10^4 \text{ cm}^{-3}$	$10^{14} \text{ cm}$	$10^{10} \text{ cm}$	0.25
0.01 pc	$10^4 \text{ cm}^{-3}$	$10^{12} \text{ cm}$	$10^{10} \text{ cm}$	$2.5 \times 10^{-5}$

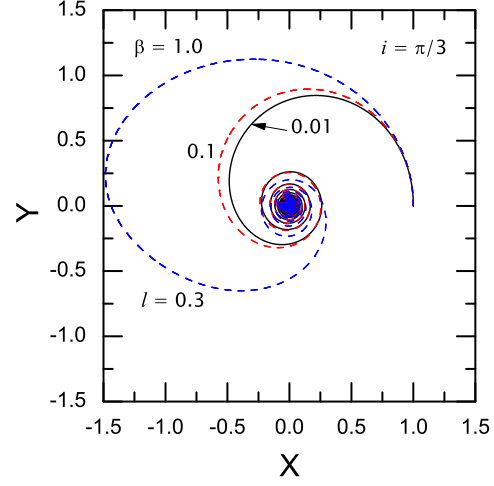


FIG. 5.— Orbit of a BLR cloud in the plane of motion for cases with different values of the parameter  $l$ . Here, we have  $\beta = 1$  and  $i = \pi/3$  and the rest of the input parameters and the initial conditions are similar to figure 2.

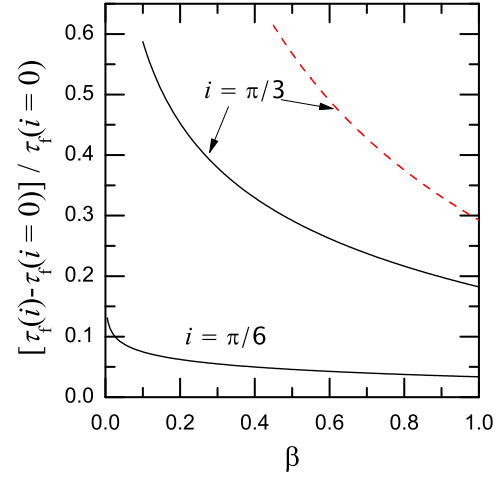


FIG. 6.— Ratio of  $[\tau_f(i) - \tau_f(i=0)] / \tau_f(i=0)$  as a function of the parameter  $\beta$  when the intercloud is static (solid) or rotating (dashed) for different inclination angles. Input parameters are  $\alpha = 0.1$ ,  $\epsilon' = 1$ ,  $\mu_m N_0 \sigma_T = 3/2$  and  $l = 0.25$ . The initial conditions are  $\tilde{r}(\tau=0) = 1$ ,  $\dot{\tilde{r}}(\tau=0) = 0$ ,  $\psi(\tau=0) = 0$  and  $\dot{\psi}(\tau=0) = 1$ . Each curve is labeled with corresponding value of  $i$ . When the intercloud is static and the inclination angle is  $i = \pi/6$  (solid), there is an increase in the time-of-flight over the case when the inclination angle is zero (i.e., radiation forces do not operate) as the dimensionless drag coefficient decreases. This enhancement in the time-of-flight is more significant for the smaller values of the dimensionless drag coefficient. Exactly the same behavior is found when the intercloud is rotating and the inclination angle is  $i = \pi/6$ , but its difference with the shown case with static atmosphere (solid) is negligible and for this reason, this particular case has not been shown here.

We now examine orbits of the BLR clouds in the plane of motion by solving the orbital equations. The background gas is rotating according to ADAF solutions. Describing the results is easier if the same initial conditions are used for all the considered cases. Thus, we assume that a cloud starts its journey from the initial location

$\tilde{r} = 1$  (note that all variables are dimensionless). The rest of the initial conditions are  $\dot{\tilde{r}}(\tau = 0) = 0$ ,  $\psi(\tau = 0) = 0$  and  $\dot{\psi}(\tau = 0) = 1$ . We found that shape of the orbits is qualitatively similar to when a linear drag is used, i.e. orbit of a BLR cloud decays due to the resistive nature of the drag force. But we can calculate the time-scale of this orbital decay when the drag force is quadratic. In doing so, time-of-flight  $\tau_f$  is defined as the time needed for traveling of a cloud from its initial location to the center. In order to determine the orbital shape of a BLR cloud and its time-of-flight, we have to adopt the input parameters consistent with the observational data. According to the observations, we have  $r_0 \sim 0.01 - 1$  pc,  $R_{\text{cl}0} \sim 10^{14}$  cm,  $n_0 \sim 10^4$  cm $^{-3}$  and  $n_{\text{cl}0} \sim 10^{10}$  cm $^{-3}$  (e.g., Rees et al. 1989; Netzer 2013; Marconi et al. 2008; Plewa et al. 2013). Tables 1 and 2 summarize our input parameters; however, in Table 2 the mass of a BLR cloud is assumed to be  $10^{-8} M_\odot$ .

Figure 2 displays orbital shape of a BLR cloud in the plane of motion (i.e.,  $XY$ -plane where  $X$ -axis is along OA in Figure 1) with inclination angles  $i = \pi/18$  (top) and  $i = \pi/3$  (bottom) for dimensionless drag coefficient  $\beta = 0.01$ . Input parameters are  $\alpha = 0.1$ ,  $\epsilon' = 1$  and  $k_0 = 0.2 \sin i$ . Also, the initial conditions are  $\tilde{r}(\tau = 0) = 1$ ,  $\dot{\tilde{r}}(\tau = 0) = 0$ ,  $\psi(\tau = 0) = 0$  and  $\dot{\psi}(\tau = 0) = 1$ . Radial distance of a cloud gradually decreases because of considering the drag force. The non-isotropic nature of the central radiation becomes more significant with increasing the inclination angle  $i$ . In Figures 3 and 4 orbital motion of clouds with the same initial and input parameters are explored but with larger values for the drag coefficient.

In our model, the effect of the radiation force on the orbit of a cloud appears through the dimensionless parameter  $k_0$  which is directly proportional to the Eddington ratio  $l$  and  $\sin i$ . Thus, radiation force operates more significantly in cases with a high inclination angle or a large Eddington ratio. In order to have bound orbits, the radiation force can not be arbitrary large and for a given set of the input parameters, however, there is always a maximum critical value of parameter  $k_0$  so that beyond this value the gravitational force is not able to keep a cloud in a bound orbit. In Figures 2-4 the orbits are shown for two values of inclination. Since radiation force pushes a cloud toward larger radii, one can expect cases with a larger inclination angle exhibit wider orbits in comparison to a case with a smaller inclination angle. This speculation has been confirmed in Figures 2-4. The effect of the Eddington ratio on the shape of orbits are explored in Figure 5 for different values of the Eddington ratio  $l$ . Here, we have  $\beta = 1$  and  $i = \pi/3$  and the remaining input parameters are similar to Figure 2. Having all the parameters fixed, we found that the orbits are no longer bound once the Eddington ratio exceeds a value around 0.3. Nevertheless, the shape of orbits is not modified significantly so long as the ratio  $l$  is roughly less than 0.1. Corresponding to the cases with  $l = 0.01, 0.1$  and  $0.3$ , the dimensionless time-of-flight is found 7.47, 7.78 and 12.75, respectively.

We explored various cases with different sets of the input parameters and the corresponding dimensionless time-of-flight  $\tau_f$  is obtained. Interestingly, we found that time-of-flight is in proportion to the inverse of the dimensionless drag coefficient  $\beta$  so the constant of the proportionality depends on the input parameters.

For a static intercloud gas, we found that  $\tau_f(i = 0) \approx 2.13/\beta^{0.89}$ ,  $\tau_f(i = \pi/6) \approx 2.20/\beta^{0.90}$  and  $\tau_f(i = \pi/3) \approx 2.52/\beta^{1.01}$ . When the intercloud is rotating, the time-of-flight is obtained as  $\tau_f(i = 0) \approx 7.38/\beta^{0.97}$ ,  $\tau_f(i = \pi/6) \approx 8.00/\beta^{0.96}$  and  $\tau_f(i = \pi/3) \approx 9.54/\beta^{1.20}$ . Except for the cases with zero inclination angle where the radiation force does not operate, however, in other cases the above fitted time-of-flight functions are not valid for the whole range of the dimensionless drag coefficient  $\beta$ . For a static intercloud gas, a BLR cloud will not be in bound orbit once the parameter  $\beta$  drops to values less than 0.005 for  $i = \pi/6$  and 0.1 for  $i = \pi/3$ . In a rotating intercloud gas, these critical values are larger so that we do not observe bound orbits when  $\beta$  is less than 0.02 for  $i = \pi/6$  and 0.43 for  $i = \pi/3$ . Figure 6 shows the ratio  $[\tau_f(i) - \tau_f(i = 0)]/\tau_f(i = 0)$  as a function of the parameter  $\beta$  when the intercloud is static (solid) or rotating (dashed) for different inclination angles.

Thus, we can write  $\tau_f \simeq \tau_0/\beta$  where  $\tau_0$  depends on the input parameters. Although the constant of proportionality  $\tau_0$  depends on the input parameters, we found that its variations with the input parameters does not affect significantly the main conclusion in our subsequent discussions. Time-of-flight for a linear drag is also proportional to inverse of the dimensionless drag coefficient, though definition of this coefficient is different from ours (see Eq.(8) in Shadmehri (2015)). One can easily confirm our approximate relation for the time-of-flight using dimensional analysis. A cloud loses its kinetic energy  $1/2mv^2$  due to the dissipative nature of the drag force with a rate equal to  $F_d v$ , where  $v$  is the velocity of the cloud and  $m$  is its mass and  $F_d$  is the drag force. Thus, time-of-flight can be written as  $(1/2mv^2)/(1/2\rho C_D \pi R_{\text{cl}}^2 v^3)$  which implies the dimensionless time-of-flight to be proportional to  $\beta^{-1}$ , i.e.  $\tau_f \propto \beta^{-1}$ .

For a cloudy BLR system around a black hole with mass  $10^8 M_\odot$ , our time unit becomes  $t_0 \simeq 1.5$  yr if we set  $r_0 = 0.01$  pc. Tables 1 and 2 show that the dimensionless drag coefficient varies from  $2.5 \times 10^{-5} C_D$  to  $25 C_D$  depending on the background gas density and the properties of a cloud such as its density and radius. Obviously, the longest cloud flight times occur when the parameter  $\beta$  is as small as permissible and the radiation force is as large as it can be. The effect of the radiation force does not appear for clouds with zero inclination angle and considering the above fitted functions for the time-of-flight, this time-scale will be between  $\tau_f(\beta = 10^{-5}) \simeq 3 \times 10^6$  yr and  $\tau_f(\beta = 10) \simeq 0.2$  yr for a static intercloud gas. These estimates are modified in a rotating background gas as  $\tau_f(\beta = 10^{-5}) \simeq 10^7$  yr and  $\tau_f(\beta = 10) \simeq 0.7$  yr. For clouds with non-zero inclination angles, however, radiation pressure force increases  $\tau_f$  as we confirmed in Figures 5 and 6. But in these cases, there is always a lower limit for  $\beta$  so that for the drag coefficient less than this critical value clouds will be pushed outward due to the strong radiation force. When the background gas is static, for example, the explored cases in Figure 6 show that the critical value of  $\beta$  is 0.005 and 0.1 for inclination angles  $\pi/6$  and  $\pi/3$ , respectively. Then, the time-of-flight becomes  $\tau_f(\beta = 0.005) \simeq 390$  yr

and  $\tau_f(\beta = 0.1) \simeq 39$  yr which are considerably shorter than the estimated  $\tau_f$  for the clouds with zero inclination angle. Critical value of  $\beta$  is larger in a system with a rotating intercloud gas and the corresponding time-of-flight is found as  $\tau_f(\beta = 0.02, i = \pi/6) \simeq 500$  yr and  $\tau_f(\beta = 0.43, i = \pi/3) \simeq 40$  yr. Using this approximate relation for the time-of-flight, we can discuss about nature of BLR clouds by comparing it with the lifetime of the whole system  $\tau_{\text{life}}$ . If  $\tau_f$  becomes shorter than  $\tau_{\text{life}}$ , all clouds will fall onto the central object and the system will be depleted of clouds unless replenishment mechanisms operate to generate new clouds. Observational evidences show that BLRs are clumpy (e.g., Rees et al. 1989), though we do not know if they are continuously forming or long-lived objects. But if  $\tau_f < \tau_{\text{life}}$ , then existence of mechanisms for generating new clouds are needed. The next step is to obtain a lower limit for the lifetime of the whole system. One can argue so long as a gas reservoir which is known as intercloud gas exists, these BLR clouds may form and move in their orbits. Thus, we can introduce the accretion time-scale as a lower limit for the lifetime of the whole system, i.e.  $\tau_{\text{life}} = M/\dot{M}$  where  $\dot{M}$  is the accretion rate. Despite of uncertainty about the geometry and the nature of the accretion in these system, an approximate relation between the Eddington ratio and the accretion rate can be written as  $l \simeq \dot{M}/\dot{M}_{\text{Edd}}$ , where  $\dot{M}_{\text{Edd}}$  is the Eddington accretion rate (see p. 40, Netzer 2013). Thus, one can obtain  $\tau_{\text{life}} \simeq 4 \times 10^8 \frac{\eta}{l}$  yr, where  $\eta \sim 0.1$  is the mass-to-luminosity conversion efficiency (Netzer 2013). Evidently, this estimated lifetime is much longer than the time-of-flight of BLR clouds except for clouds with zero inclination angle which may have  $\tau_f \sim \tau_{\text{life}}$  under very restrictive circumstances. This implies that mechanisms for continuous formation of BLR clouds should operate even when the drag force is quadratic. In the absence of such cloud creation mechanisms, however, it seems only clouds with orbital plane near to equatorial plane may survive and the rest of the clouds will fall onto central black hole very quickly and thereby, a disc like configuration for the geometry of spatial distribution of BLR clouds is expected (also see, Khajenabi 2015).

Although our model is based on the existence of an ensemble of discrete independent clouds in BLRs, more recent evidence may suggest that the system is not clumpy as has been studied by Arav et al. (1998) in their attempt to find direct signature of discrete clouds in BLR of the Seyfert galaxy NGC 4151. They argued that BLRs are not made of independent clouds. Our analysis shows that even if BLR clouds do exist, they can not be long-lived due to the effect of the drag force. In the absence of a clear physical understanding of possible mechanisms for continuous formation of BLR clouds, however, it seems the system should be depleted of clouds which is consistent with the recent observations (Arav et al. 1998).

We note that our analysis is based on an assumption which states that the clouds are in pressure equilibrium with their ambient medium. This constraint should not lead to unphysical values for the ratio of density of cloud to the intercloud density, i.e.  $\rho_{\text{cl}}/\rho$ , which scales as the ratio of inter-cloud medium to cloud temperature. Since mass of cloud  $m$  is conserved during its journey, we obtain  $\rho_{\text{cl}} = \rho_{\text{cl0}}(r/r_0)^{-5/2}$  where  $\rho_{\text{cl0}} = 3m/(4\pi R_{\text{cl0}}^3) \sim 10^{10} \text{ cm}^{-3}$ . Having equation (2) for the intercloud density, we obtain  $\rho_{\text{cl}}/\rho = \rho_{\text{cl0}}/\rho_0(r/r_0)^{-1}$  or  $\rho_{\text{cl}}/\rho \sim 10^6(r/r_0)^{-1}$  which means the ratio of the densities can not be arbitrary large so long as a cloud is not very close to the central parts.

#### 4. CONCLUSION

Our goal is to analyze orbits of BLR cloud subject to a drag force proportional to the velocity square. We calculated time-of-flight of the clouds for different initial conditions including motion through a static and rotating atmospheres. In all cases, however, we found that a system is generally older than typical time-scale of spiraling a cloud onto the central region. It means without mechanisms for continuous creation of clouds, a typical BLR system will eventually depleted of clouds. But this feature is not supported by observations. Thus, we can conclude BLR clouds are constantly forming.

I am very grateful to referee for his/her constructive report which greatly improved the quality of this paper.

#### REFERENCES

- Arav, N., Barlow, T. A., Laor, A., Sargent, W. L. W., & Blandford, R. D. 1998, *MNRAS*, 297, 990  
 Blumenthal, G. R. & Mathews, W. G. 1975, *ApJ*, 198, 517  
 —. 1979, *ApJ*, 233, 479  
 Capriotti, E., Foltz, C., & Byard, P. 1979, *ApJ*, 230, 681  
 —. 1980, *ApJ*, 241, 903  
 —. 1981, *ApJ*, 245, 396  
 Carroll, T. J. & Kwan, J. 1985, *ApJ*, 288, 73  
 Fromerth, M. J. & Melia, F. 2001, *ApJ*, 549, 205  
 Gillessen, S., Genzel, R., Fritz, T. K., Quataert, E., Alig, C., Burkert, A., Cuadra, J., Eisenhauer, F., Pfuhl, O., Dodds-Eden, K., Gammie, C. F., & Ott, T. 2012, *Nature*, 481, 51  
 Khajenabi, F. 2015, *MNRAS*, 446, 1848  
 Krause, M., Burkert, A., & Schartmann, M. 2011, *MNRAS*, 411, 550  
 Krause, M., Schartmann, M., & Burkert, A. 2012, *MNRAS*, 425, 3172  
 Kwan, J. & Carroll, T. J. 1982, *ApJ*, 261, 25  
 Liu, Y. & Zhang, S. N. 2011, *ApJL*, 728, L44  
 Marconi, A., Axon, D. J., Maiolino, R., Nagao, T., Pastorini, G., Pietrini, P., Robinson, A., & Torricelli, G. 2008, *ApJ*, 678, 693  
 Mathews, W. G. 1974, *ApJ*, 189, 23  
 —. 1986, *ApJ*, 305, 187  
 Mathews, W. G. & Veilleux, S. 1989, *ApJ*, 336, 93  
 McCormick, B. W. 1979, *Aerodynamics, Aeronautics, and Flight Mechanics*  
 McCourt, M. & Madigan, A.-M. 2015, *ArXiv e-prints*  
 Namekata, D., Umemura, M., & Hasegawa, K. 2014, *MNRAS*, 443, 2018  
 Narayan, R. & Yi, I. 1994, *ApJL*, 428, L13  
 Netzer, H. 2013, *The Physics and Evolution of Active Galactic Nuclei*  
 Netzer, H. & Marziani, P. 2010, *ApJ*, 724, 318  
 Osterbrock, D. E. & Mathews, W. G. 1986, *Ann. Rev. Astron. Astrophys.*, 24, 171  
 Pfuhl, O., Gillessen, S., Eisenhauer, F., Genzel, R., Plewa, P. M., Ott, T., Ballone, A., Schartmann, M., Burkert, A., Fritz, T. K., Sari, R., Steinberg, E., & Madigan, A.-M. 2015, *ApJ*, 798, 111  
 Plewa, P. M., Schartmann, M., & Burkert, A. 2013, *MNRAS*, 431, L127  
 Rees, M. J. 1987, *MNRAS*, 228, 47P  
 Rees, M. J., Netzer, H., & Ferland, G. J. 1989, *ApJ*, 347, 640  
 Shadmehri, M. 2014, *MNRAS*, 442, 3528  
 —. 2015, *MNRAS*, 451, 3671